Simulation Study of Prostate Tissue Ablation by Pulsed Nd:YAG, Ho:YAG and Thulium Fiber Surgical Lasers with Minimum Carbonization Effect

Munqith S. Dawood
Medical Engineering Department
Collage of engineering, Al-Nahrain University
E-mail: monkithsdz51@yahoo.com

Haider Monaf
Ministry of Health

Abstract

The laser-tissue interaction and its thermal effects depend on the parameters of both of the tissue and the used laser. In this paper the laser ablation efficiency of prostate tissue has been studied theoretically by using pulsed Nd:YAG, Ho:YAG and Thulium fiber surgical lasers. Different levels of energies were considered for these lasers, which operate in 20 and 40 Hz pulse repetition frequencies (prf) to evaluate the prostate tissue temperature rise up to the required ablation state. The Gambit program was used first to simulate the geometrical shape of the treated prostate tissue, then the radiative transfer equation (RTE) of the ANSYS Fluent program was applied to simulate and solve the ablation process equations. The results showed that the low rates of repetition frequencies and low laser energies increase the allowed time for safe ablation operation before reaching the carbonization state. It was found also that although the Ho:YAG laser vaporizes prostate tissue faster than the Thulium fiber laser did, the pulsed Thulium fiber laser produced much lower temperature side effects like coagulation, hyperthermia and carbonization of the rest of the prostate tissue, which is surrounding the ablated zone for the same applied average powers by the other two lasers.

Keywords: Ho:YAG laser; Nd:YAG laser; Thulium fiber laser; prostate tissue ablation; ANSYS software; Gambit program.

1. Introduction

The laser surgeries have the potential to revolutionize many traditional surgical operations and tools used for cutting and removing layers or slices of some biological tissues and cancerous tumors [1, 2]. This laser potential is rooted in the three following features [3, 4]:

1) The ability to produce short pulses of high intensity narrow beam light;

2) The ability to deliver this light precisely to the target tissue in the body; and

3) The ability to selectively affect one tissue type over another.

In laser surgery, the high laser energy rises up the tissue temperature and consequently vaporizes and cut off the tissues like a scalpel [5].

The laser wavelength and its mode of operation parameters are considered in this simulation study due to their importance in the laser- prostate tissue interactions [6,7]. The simulation is directed to understand the resulting tissue thermal response and the increase of its temperature after each laser impulsive heat deposition in the tissue to follow up its ablation process.

Three widely used surgical lasers are selected for this study. They are the Holmium:YAG laser (λ = 2120nm); Nd:YAG laser (λ = 1064 nm) and Thulium fiber laser (λ= 1908) [7-9]. The energies of these lasers are absorbed by the water inside the cells of the desired tissue, which leads to their rapid vaporization due to the significant increase of their temperature [6,10]. In this paper we present the model of numerical mathematical calculations, combining the laser parameters and the biological tissue parameters with the equations of the radiation transfer and heat distribution within the ANSYS software programs. The results introduce the comparative effectiveness of these lasers in the non carbonized laser prostate tissue ablation depths, volumes and the rate of its temperature rise when they operate in their pulse modes.

2. Materials and methods

The degree and extent of the laser energy transformation into thermal effect within the prostate tissue depend on the mode parameters of the used laser and on the optical, geometrical and thermal properties of the tissue [11-13]. Figure (1) shows schematically the general process of the laser thermal interaction with tissues. The prostate tissue absorbs the laser energy during the transportation of this light through its turbid media. This absorption of energy rises up the prostate tissue temperature, which will propagate by conduction within tissue to produce the necessary heat required for ablation. The convection effect by blood and urine was neglected in this study.

For each applied laser energy, the temperature rise up of the treated prostate area and the resulted heat distribution within the mass of prostate tissue

was calculated by using the numerical solutions of the radiation transfer equation (RTE), which governed the light transport in a turbid media like the prostate tissue. The Fluent programs of the general ANSYS software programs were used.

To simulate the prostate tissue geometry, a finite number of discrete solid angles was created as a mesh by using Gambit program. The finite-volume scheme and its extension has been used to construct the meshes in the solution process. Each one of these solid angles is associated with a vector direction fixed in the global Cartesian system (x, y, z). By selecting the uncoupled case option in the fluent program, the equations for the energy and radiation intensities were solved one by one by this program.
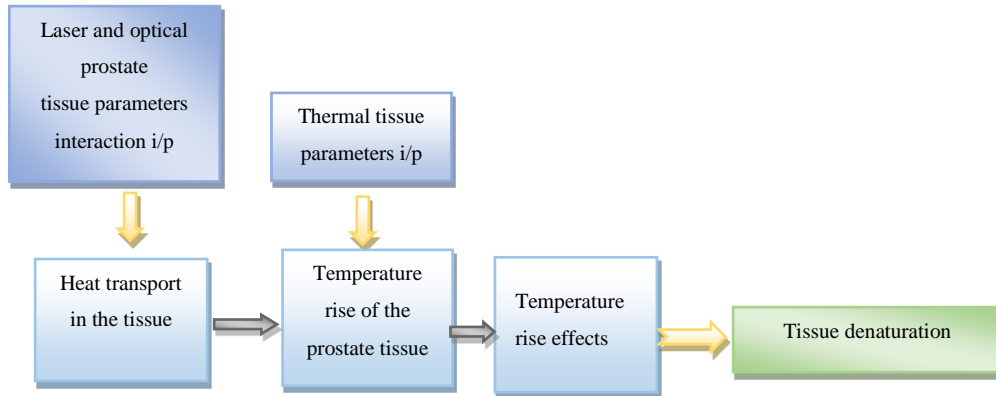

Figure 1: Flow chart of the laser- prostate tissue thermal interaction modeling.

2.1 Modeling of the prostate tissue geometry

To draw the results of temperature distributions calculations within the prostate tissue after absorbing the laser energy, it is necessary to draw first the geometrical shape of the prostate tissue. In this simulation the prostate tissue, for simplicity was considered to have a circular cross-sectional area, which consists of small triangles grid elements as shown in figure (2). This geometry was created by using Gambit software version 2.2.30. The illuminated prostate area by the laser spot on this simulated prostate tissue is called the active zone. The rest of the prostate tissue, which is surrounding the active zone is called the boundary zone.
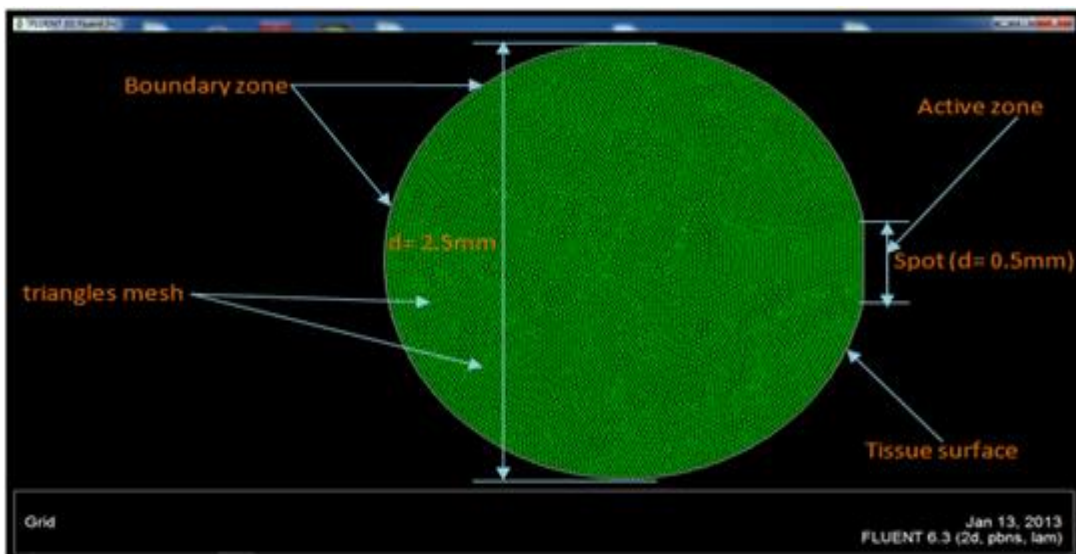

Figure 2: The suggested prostate geometry created by Gambit software in this simulation.

2.2 The prostate tissue and laser parameters

The high fluid contents (75–90%) in the biological tissues make their properties close to that of water. This means that the thermal properties of water can be used for approximate thermal calculations of laser prostate and prostate cancerous ablation. The thermal properties of the prostate tissue and its cancer was considered very close to each other [14-16].

The used prostate and laser parameters in this simulation are listed in table (1). The initial temperature of the prostate tissue (boundary zone) is considered to be 37 C^o. The propagation of heat from the illuminated zone to the surrounding prostate tissues is characterized by its thermal conductivity (k), the specific heat capacity (C) and the density (ρ) of the prostate. The prostate absorption of the laser energy is strongly depending on the wavelengths (λ) of the incident lasers radiations [6-7,17-19]. The effects of pulse repetition rate (prf), pulse duration, power (p_o), intensity (I_o) and the spot size radius (d/2) of the used laser beams were studied also by using the principal equations of laser power and intensity [20].

The intensity of the laser beam considered to fall down to $1/e^2$ of its incident value according to Gaussian distribution at the laser spot radius = waist of the beam ω.

Table 1: Optical and thermal parameters of the human prostate, which were used in the numerical simulation corresponding to each of the used laser wave lengths.

Parameter	Unite	Value	References
Specific heat capacity	Cp [J.kg^{-1}.K^{-1}]	3662	[8]
Density	ρ [kg.m^{-3}]	1060	[8]
Thermal conductivity	k [W.m^{-1}.K^{-1}]	0.512	[8]
Refractive index	N	1.33	[9]
Absorption coefficient (for λ =1064nm)	cm^{-1}	0.6	[9]
Scattering coefficient (for λ =1064nm)	cm^{-1}	110	[9]
absorption coefficient(for λ =2120nm)	cm^{-1}	36	[9]
absorption coefficient(for λ =1908nm)	cm^{-1}	120	[4]

The scattering coefficients of the Ho:YAG and the Thulium fiber lasers are neglected due to their very high absorption coefficients in comparison with the Nd:YAG laser.

2.3 Radiation Transfer Equation RTE

The collimated laser light energy falling on a turbid tissue suffers a redistribution of its intensity inside the tissue medium due to the scattering and the absorption of light in the tissue medium.

To simplify the solution of the propagating light energy through the turbid medium, it is useful to ignore some wave characteristics of light, such as polarization and interference, and considering only the flow of energy through the media. This is essentially the idea of radiative transfer theory. This theory proposes that the light transport in an absorbing and scattering turbid media (tissue) is governed by the radiative transfer equation (RTE) for a position $\vec{r}$ in a direction $\vec{s}$ in the tissue as follows [11]:

$$\frac{dI(\vec{r},\vec{s})}{ds} + (a + \sigma_s)I(\vec{r},\vec{s}) = an^2 \frac{\sigma T^4}{\pi} +$$

$$\frac{\sigma_s}{4\pi} \int_0^{4\pi} I(\vec{r},\vec{s}) \phi(\vec{s},\vec{s'}) d\Omega' \qquad ….. (1)$$

Where

$\vec{r}$ = position vector;

$\vec{s}$ = direction vector;

$\vec{s'}$ = scattering direction vector;

s = path length;

a = absorption coefficient;

n = refractive index;

σ_s = scattering coefficient;

σ = Stefan-Boltzmann constant (5.672×10^{-8} W/m^2-K^4);

I= radiation intensity, which depends on position ($\vec{r}$) and direction ($\vec{s}$);

T = local temperature;

ϕ= phase function;

Ω'= solid angle.

The RTE ignores the wave and particle characteristics of light.

2.4 The heat distribution equation in tissue

The heat transfer is achieved in general due to four physical phenomena, which are the: conduction, convection, evaporation, and radiation, but in tissue the heat transfers mainly

147

by conduction and convection. The deposited energy of light was described by the following well-known bioheat transfer equation (Pennes equation)[12, 21- 23]:

$$C_p.\frac{\partial T(r,t)}{\partial t} - \nabla.(k.\nabla T_{(r,t)}) = w_b.C_p.[T_b - T_{(r,t)}] + Q_{abs(r,t)} + Q_{met} \qquad ..... (2)$$

Where T is the temperature (K°);
C_p is the heat capacity (J.mm⁻³.K°⁻¹);
k is the thermal conductivity of tissue (W.mm⁻¹.K°⁻¹);
w_b is the blood flow rate (ml.g⁻¹.min⁻¹);

T_b is the blood temperature ;
t is time (s);
Q_{abs} is the heat source (W.mm⁻³);
Q_{met} is the metabolic heat source (W.mm⁻³).

The heat generated due to the metabolic activities of alive tissue and the effects of arterial blood flow are neglected for simplification. The calculations process of the laser - prostate tissue ablation is shown in fig (3) in block diagram form.

The procedures of temperature rise calculations of the prostate tissue and the contours drawings flowcharts are presented in figures (4 and 5).
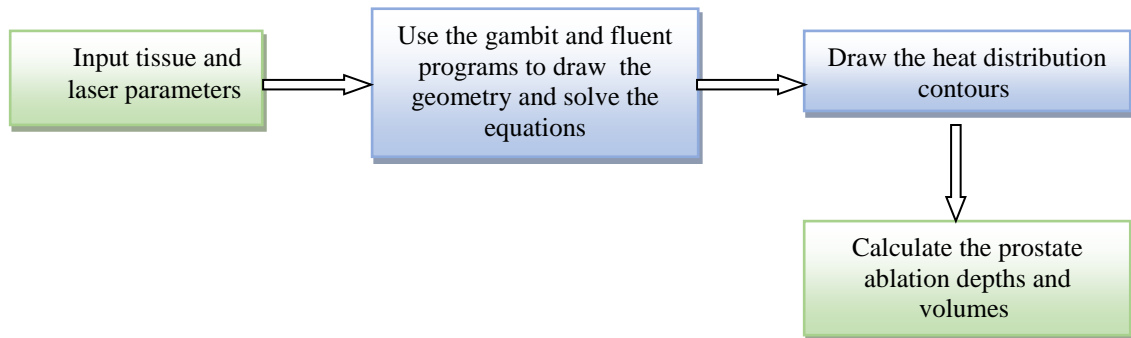
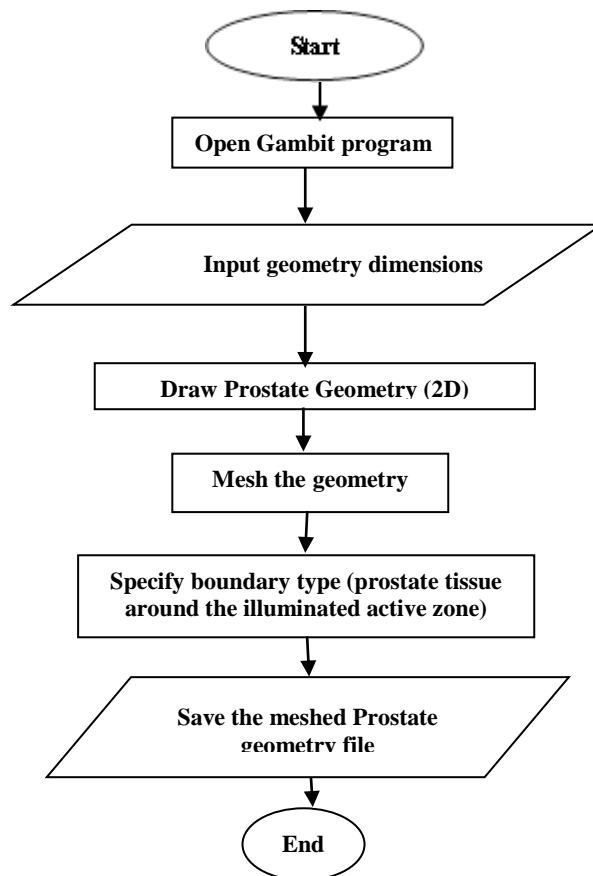**Figure 3:** Block diagram of the calculations process in this simulation.

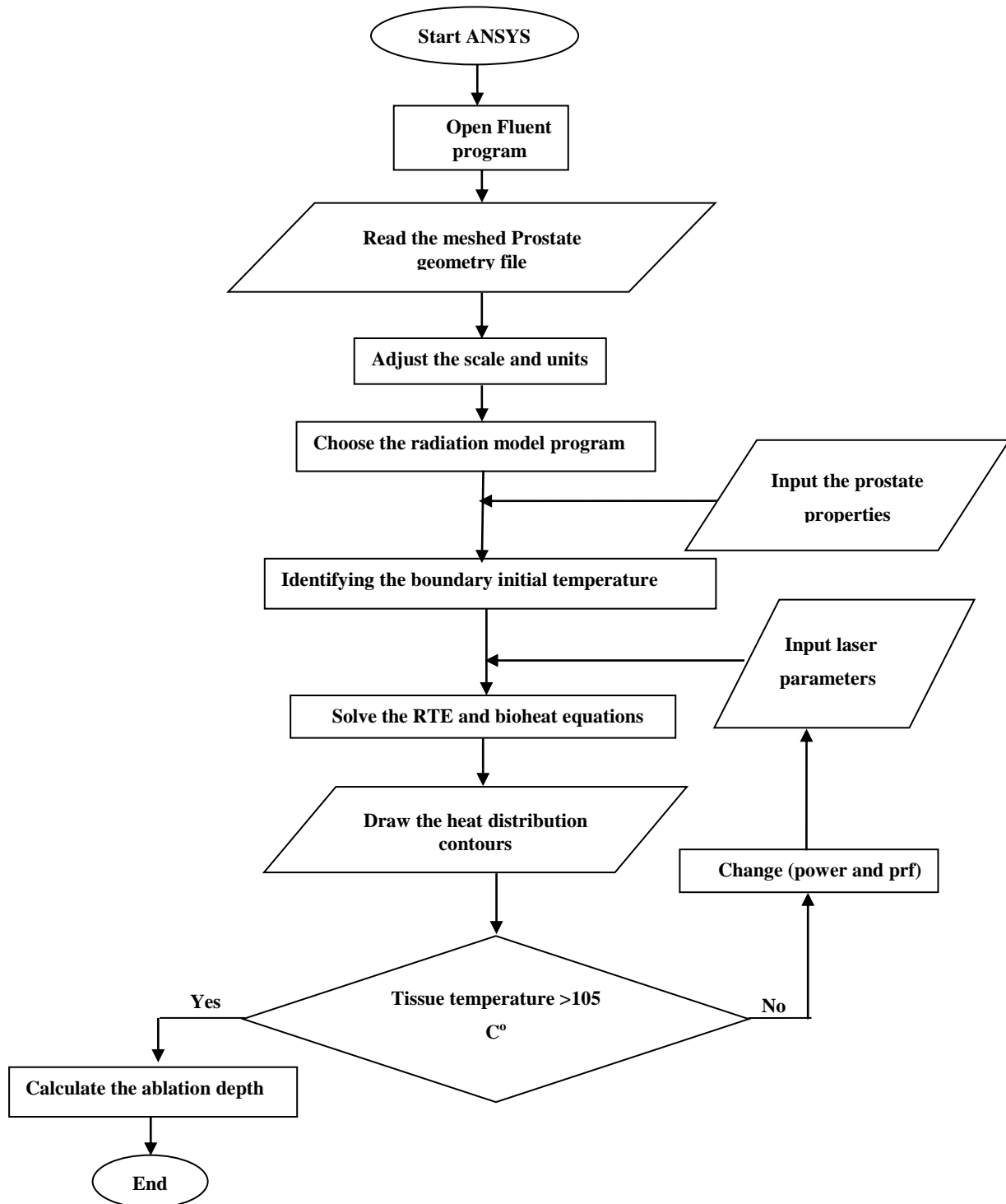**Figure 4:** Flow chart of GAMBIT program steps to draw the prostate tissue mesh.

Figure 5: Flow chart of the calculations procedure and the drawing of heat distribution contours steps used in this simulation.

3. Results
3.1 Single pulse operation

The used laser parameters in these simulation calculations are shown in table (2).

Table 2: Parameters of the used Nd:YAG; Ho:YAG and Thulium fiber lasers.

Type of laser	Wave length (nm)	Spot diameter of the laser (mm)	Pulse duration (ms)	Mode of operation
Nd:YAG	1064	0.5	(0.25-6)	Single pulse
Ho:YAG	2120	0.5	(0.25- 5)	Single pulse
Thulium fiber	1908	0.5	(0.25-2).	Single pulse

The temperature response of prostate tissue is variable according to the absorption coefficient of each laser and also according to the laser parameters like pulse repetition frequency (prf), pulse duration, pulse energy and other parameters.

The calculations results for the temperature rise rates in the prostate tissue for a single pulse of different durations and energies of the used Nd:YAG, Ho:YAG and Thulium fiber lasers are shown in the series of figures (6 to 9).
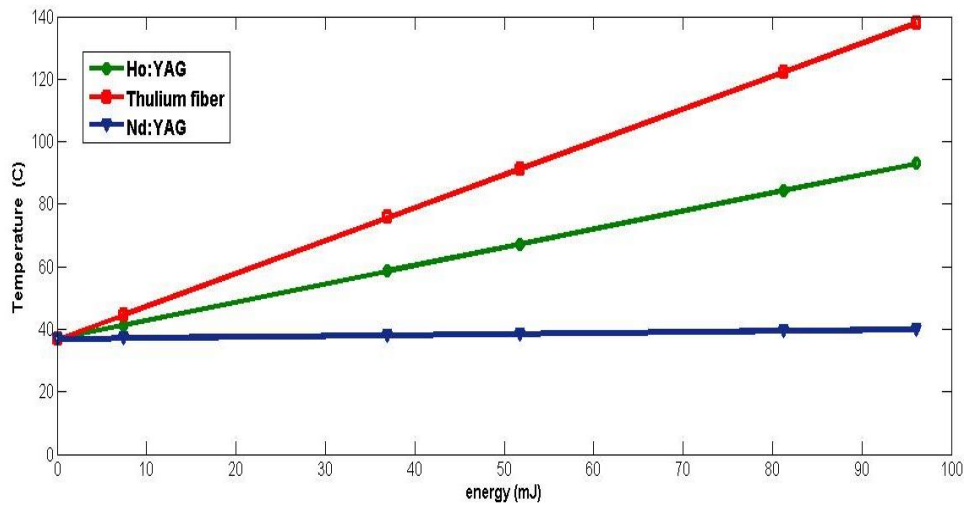

Figure 6: Prostate temperature rise due to a long single pulse duration of 100 ms of Ho:YAG, Thulium fiber and Nd:YAG lasers operating at different energies.
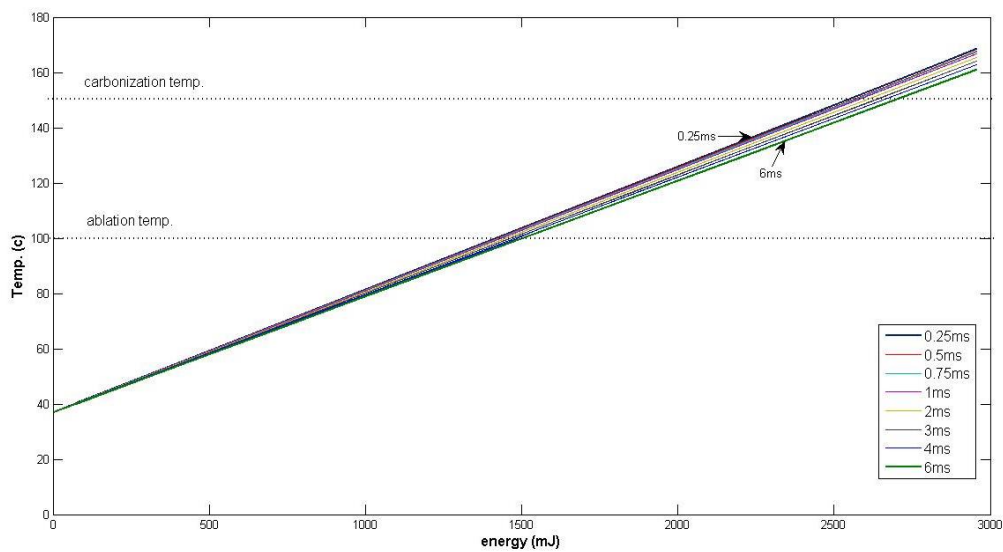

Figure 7: Temperature rise of prostate tissue due to the absorption of a single pulse of different Nd:YAG laser energies for different short pulse durations (0.25- 6) ms .
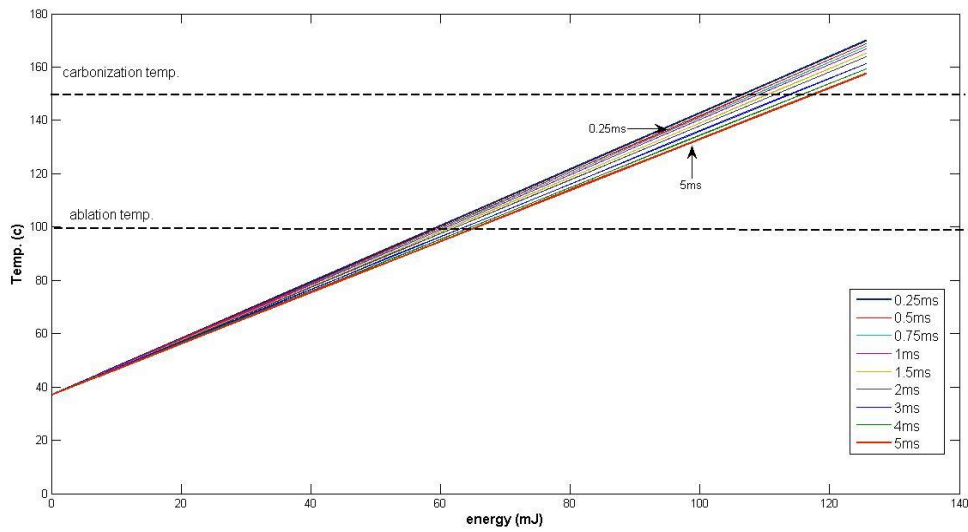
Figure 8: Temperature rise of prostate tissue due to the absorption of a single pulse of different Ho:YAG laser energies for different short pulse durations (0.25- 5) ms .
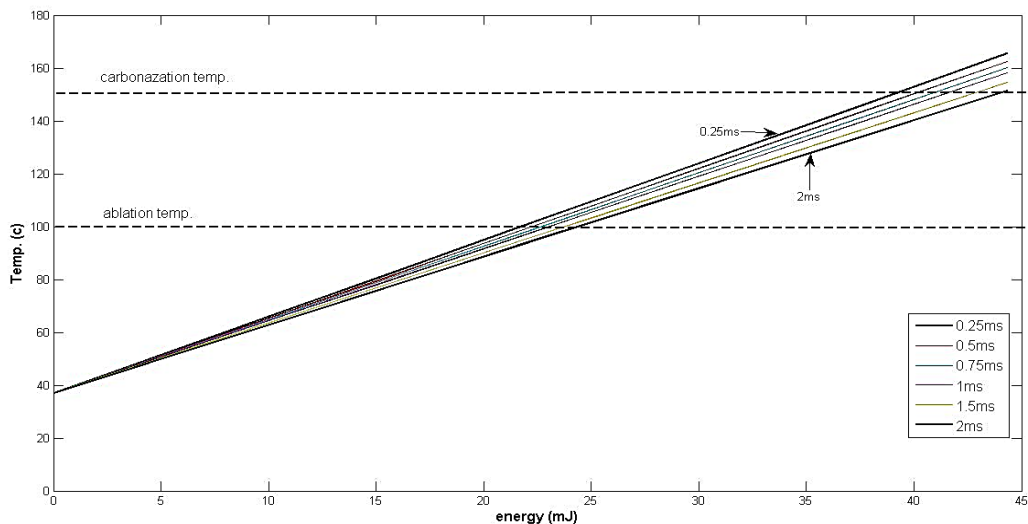

Figure 9: Temperature rise of prostate tissue due to the absorption of a single pulse of different Thulium fiber laser energies for different short pulse durations (0.25- 2) ms .

Referring to the results shown in figures (7,8 and 9), the average threshold energy necessary to start the ablation by each laser are considered to be 1550, 65 and 25 mJ for one pulse shot of the Nd:YAG, HO:YAG and Thulium fiber lasers respectively. These threshold values of energies were used, as explained by the flowchart sequence in figure (5), to draw the temperature rise distribution contours in the prostate tissue which are shown in figures (10,11,12).

These figures were analyzed by using the AutoCAD program to scale and measure the $\geq 105^{\circ}C$ temperature contours gradient depths to find out the ablation depths and their volumes for the same used threshold energies. The results of one spot ablation depths by single pulse shot according to the change of the lasers pulse durations are presented in fig. (13).
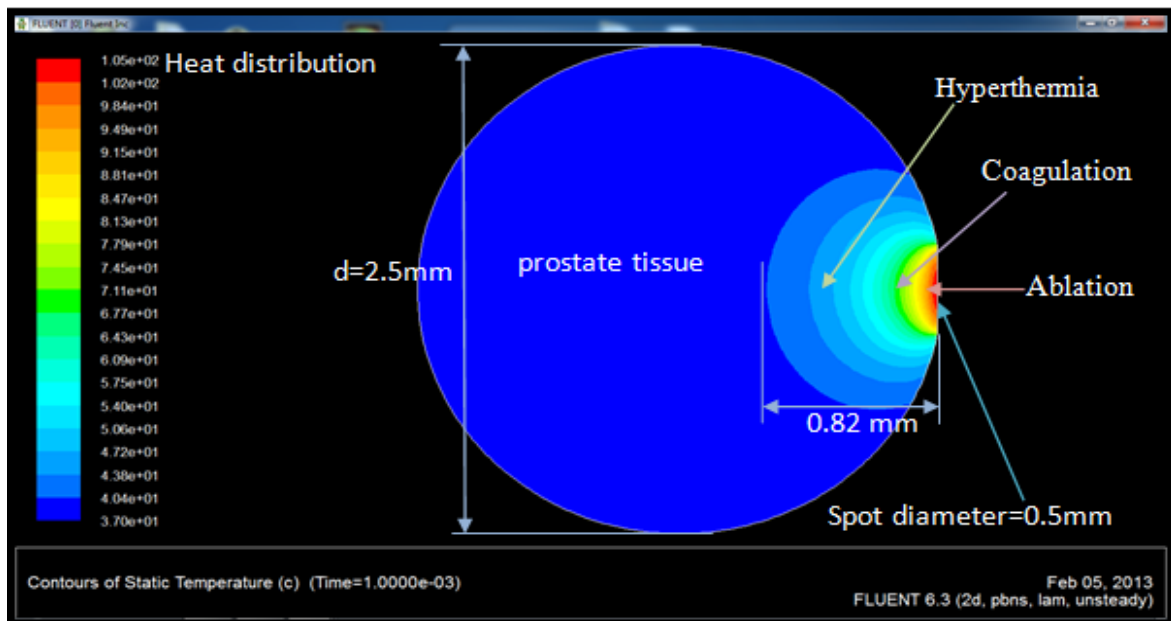
Figure 10: Heat distribution contours resulted due to the prostate tissue absorption of a single 1ms pulse of 1550 mJ energy Nd:YAG laser . The laser spot size diameter is 0.5 mm.
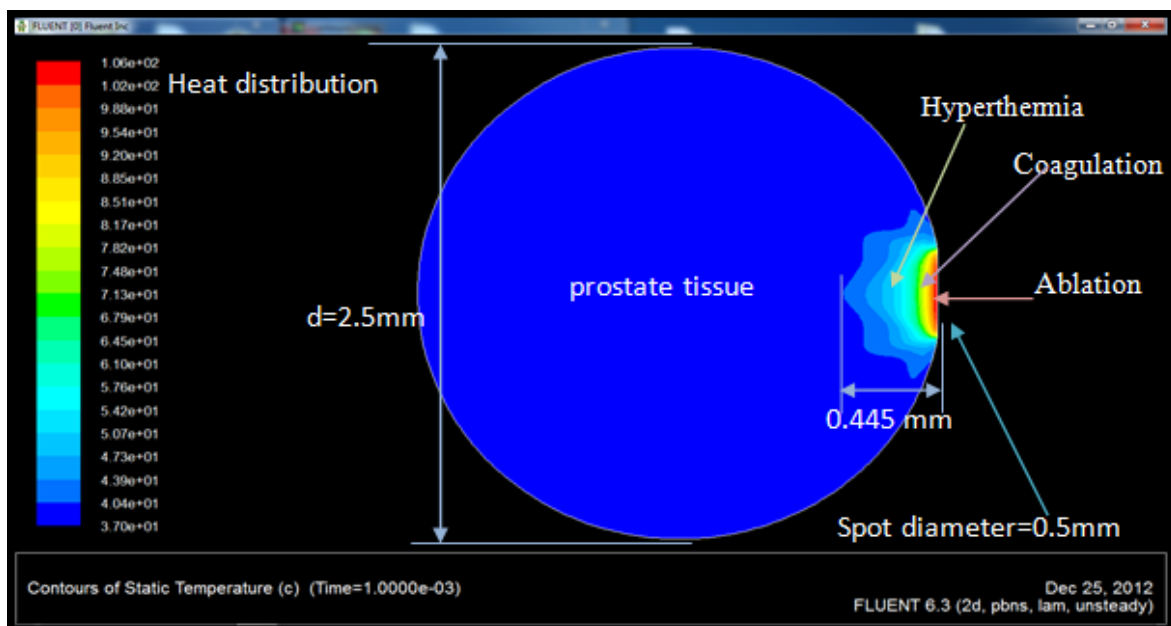

Figure 11: Heat distribution contours resulted due to the prostate tissue absorption of the Ho:YAG laser after one pulse of 1ms duration and 65 mJ energy. The laser spot size diameter is 0.5 mm.
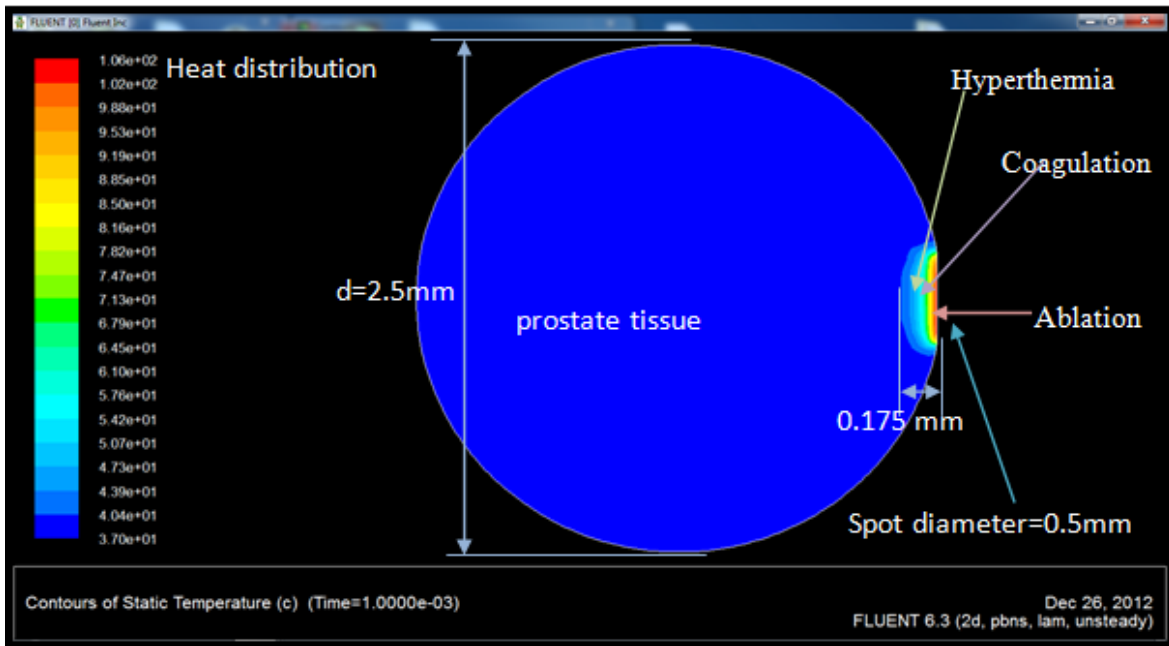
Figure 12: Heat distribution contours resulted due prostate tissue absorption of a single 1 ms pulse of 25 mJ energy of Thulium fiber laser. The laser spot size diameter is 0.5 mm.
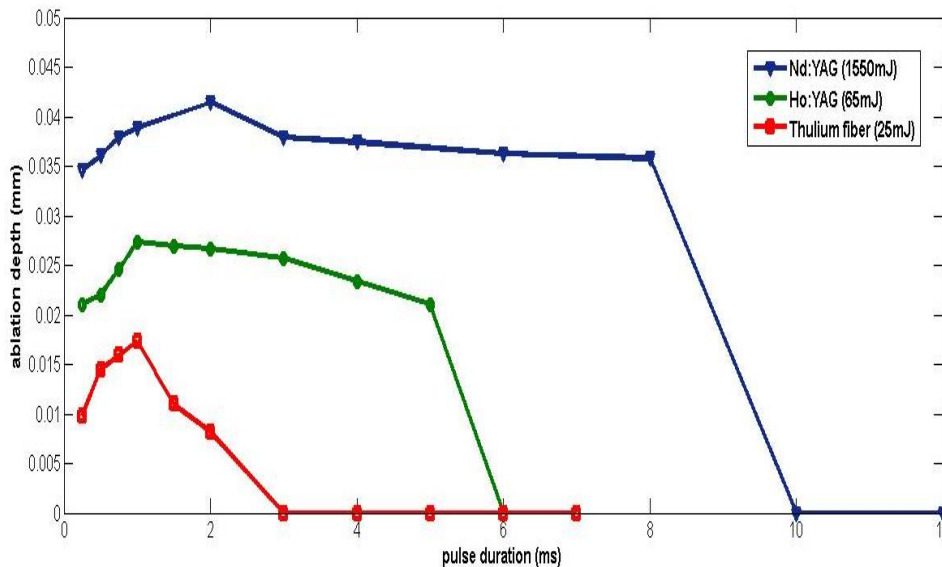

Figure 13: The calculated ablation depths in one spot prostate tissue due to the absorption of different durations of a single pulse of 1550mJ Nd:YAG; 65mJ Ho:YAG and 25 mJ energy Thulium fiber lasers.

3.2 The 20 and 40 pulse repetition frequencies (prf) operation

The rise of the prostate tissue temperature is proportional to the used laser and to the changes in its parameters. The achieved results showed that the Ho:YAG and the Thulium fiber lasers are more efficient and required much lower energies for ablation than the Nd:YAG laser did. For this reason we proceed this study without the Nd:YAG laser.

The effects of changing the prf of the pulsed Ho:YAG and Thulium fiber lasers on the prostate ablation depths and volumes were studied in this simulation for 20 Hz and 40Hz prfs. The optical properties of the treated prostate tissue assumed not changing during the operation.

From the results of many sub calculations of the minimum lasers energies required to achieve the non carbonization ablation, we select the 60,80 and 100 mJ Ho:YAG laser energies and the 40,60 and 80mJ Thulium fiber laser energies to continue studying the effect of changing only the prf of these two lasers. These energies with the other used lasers parameters are shown in table (3).

Table 3: The used parameters of the 20 and 40 Hz prf of the pulsed Ho:YAG and Thulium fiber lasers.

Pulse repetition rate	Wave length (nm)	Laser type	Laser spot siz (mm)	Energy (mJ)	Pulse duration (ms)
20 Hz	2120	Ho: YAG	1	(60, 80and100)	0.5
40 Hz	2120	Ho: YAG	1	(60, 80and100)	0.5
20Hz	1908	Thulium fiber	1	(40, 60and 80)	0.5
40Hz	1908	Thulium fiber	1	(40, 60and 80)	0.5

For comparison purposes, we chose the calculations results of the temperature rise for the lowest levels of laser energies 60mJ and 40mJ (as indicated in table (3)) for both of the Ho:YAG and Thulium fiber lasers respectively. The change of the optical properties of the tissue during the operations is not considered to simplify the calculations. The effects of changing only the pulse repetition frequency (RR) on the prostate tissue temperature rise are shown in figures (14) and (15) for the Ho:YAG and Thulium fiber lasers respectively .
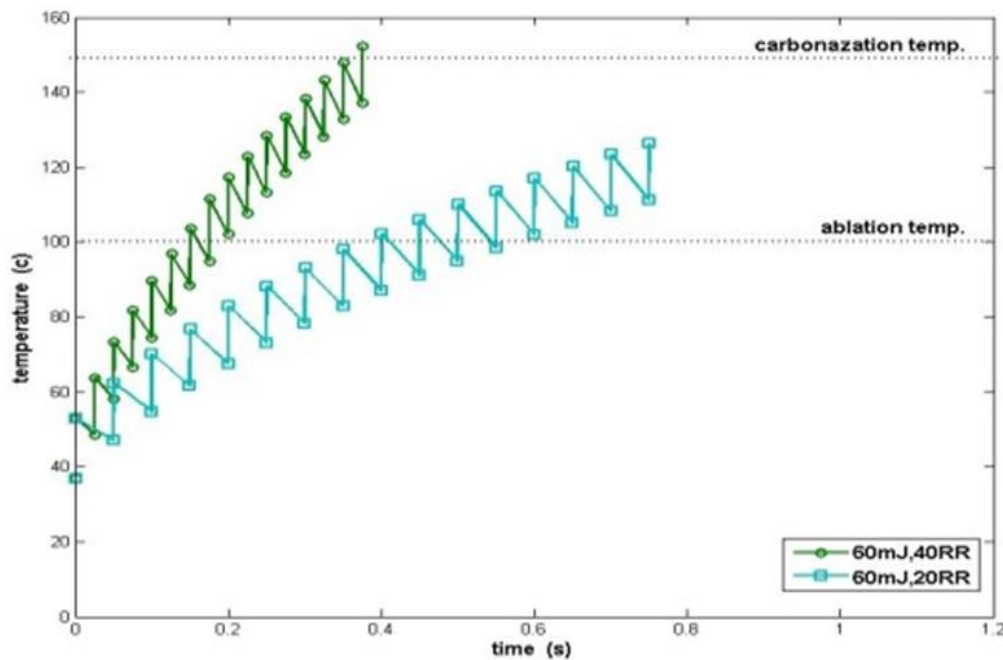

Figure 14: The rate of prostate temperature rise by 20 Hz and 40Hz prf of 60mJ, Ho:YAG laser.
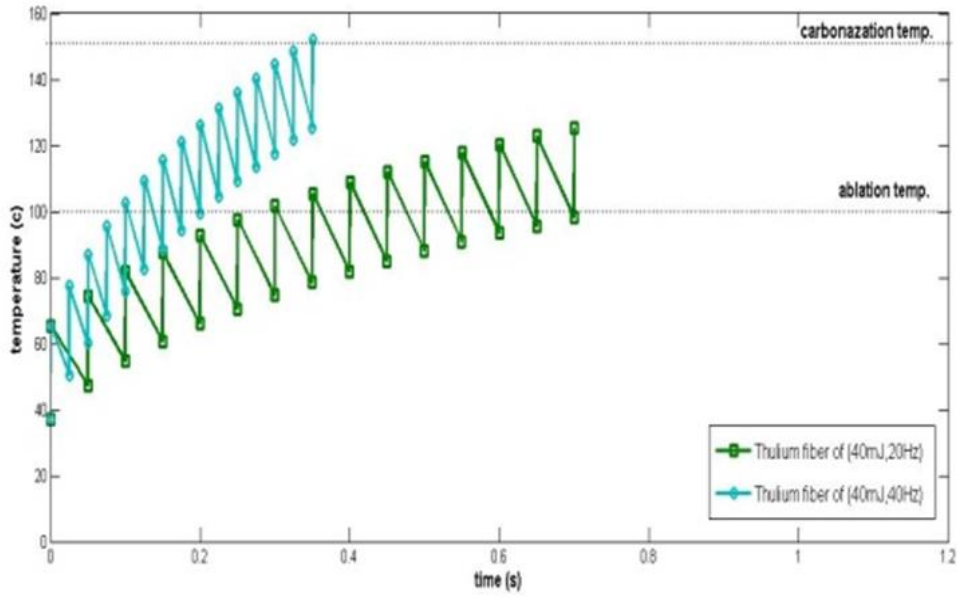
Figure 15: Temperature rise versus time by 20 Hz and 40Hz prfs of the 40mJ energy Thulium fiber laser.

The resulted non carbonized ablation depths of the prostate tissue and their volumes by applying the 60,80 and 100mJ are calculated according to the analysis and scaling of their temperature contours.The results are shown in figures (16-19) for the three selected energies of the Ho:YAG and the Thulium fiber pulsed lasers as they are appeare in table (3).
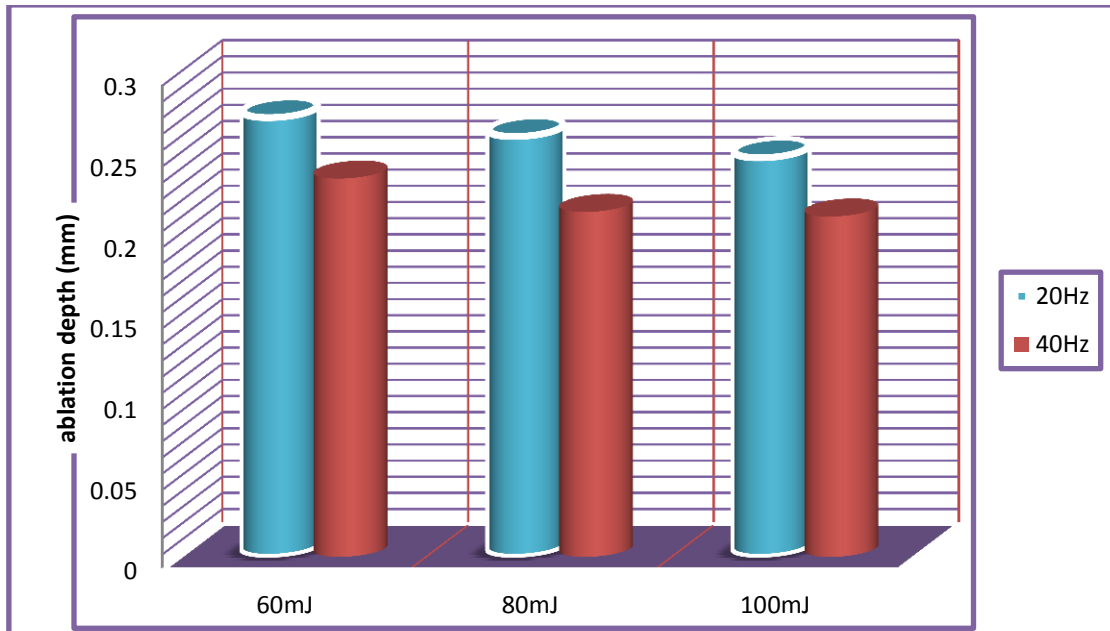

Figure 16: The non-carbonized ablation depths for 20 and 40 repetition rates of Ho:YAG laser operating at different energies.
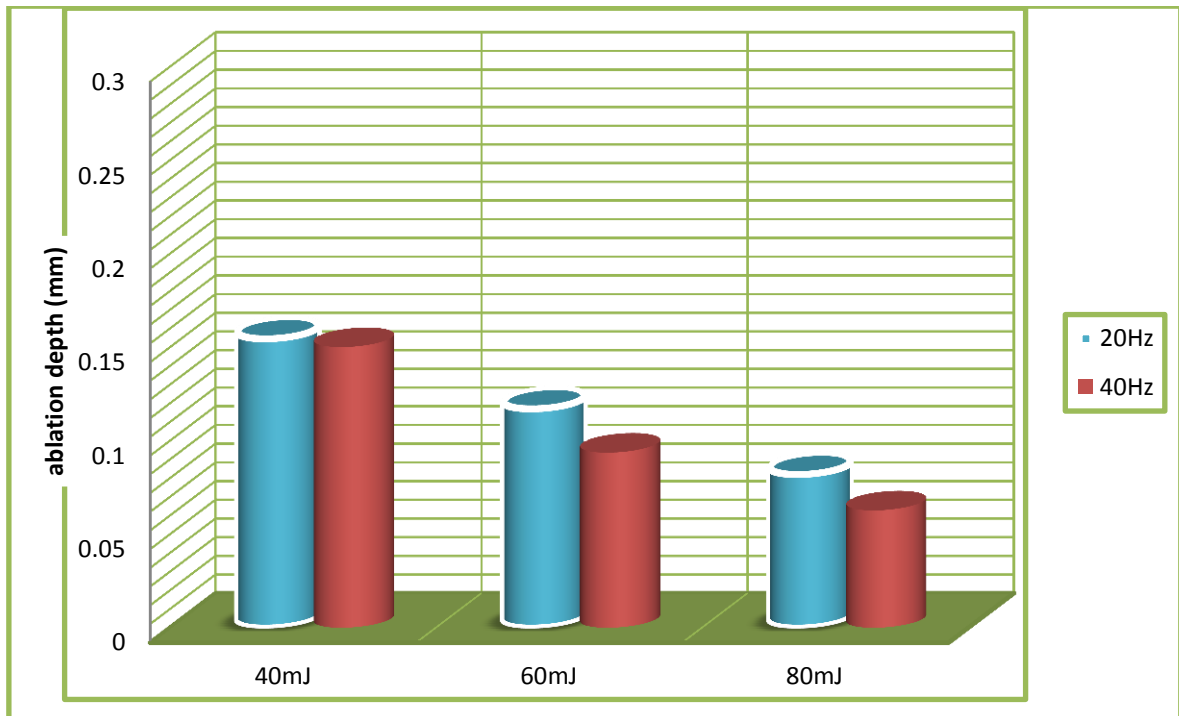
Figure 17: The calculated non carbonized ablation depths for the 20 and 40 repetition rates of the pulsed Thulium fiber laser operating at the 40, 60 and 80mJ energies.
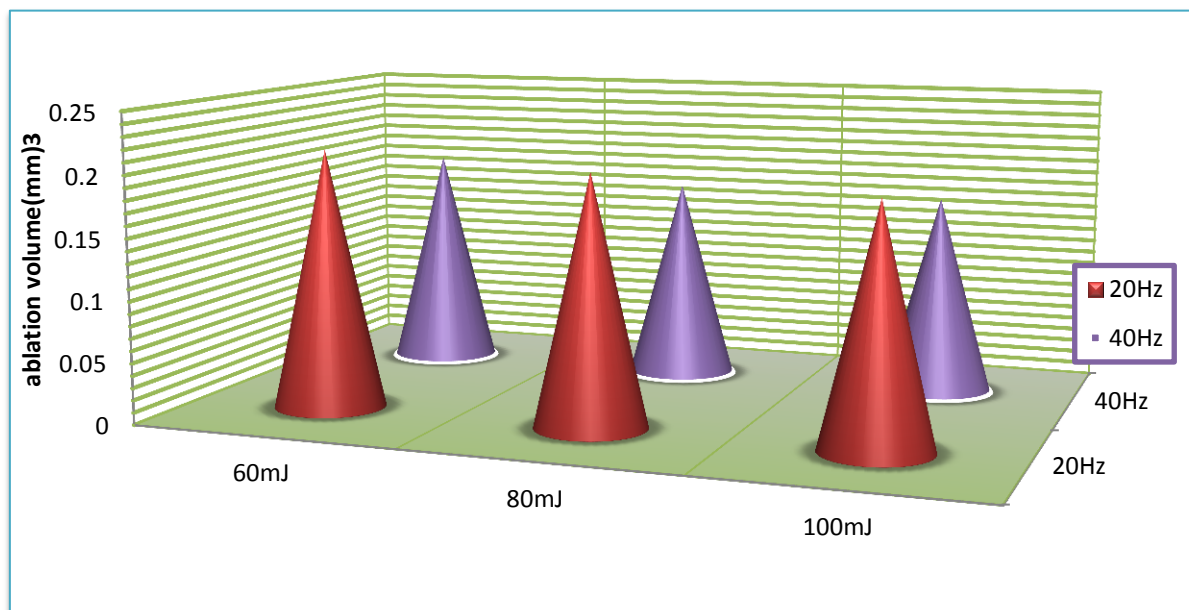

Figure 18: The non-carbonized ablated prostate volumes for the 20 and 40 repetition rates of the three Ho:YAG laser energies.
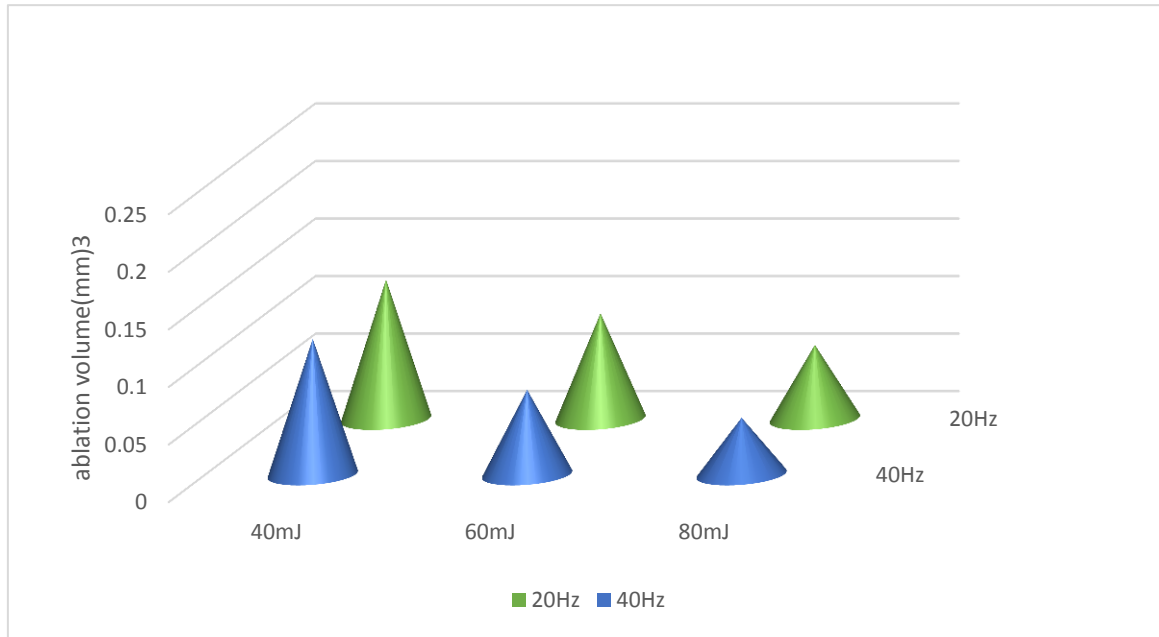
Figure 19: The non-carbonized ablation volumes made by the 20 and 40 prf pulsed Thulium fiber laser operating at the 40, 60 and 80mJ energies.

To illustrate a direct and fast comparison, the calculated ablation depths rates which were made by the pulsed Ho:YAG and the pulsed Thulium fiber lasers operating at 20 and 40 Hz prfs are shown in figures (20) and (21) for their 60mJ common energy.

Figure 20: Ablation depths rates made by 20 Hz prf pulsed Ho:YAG and Thulium fiber lasers. The operating energy is 60mJ for both of the two lasers.

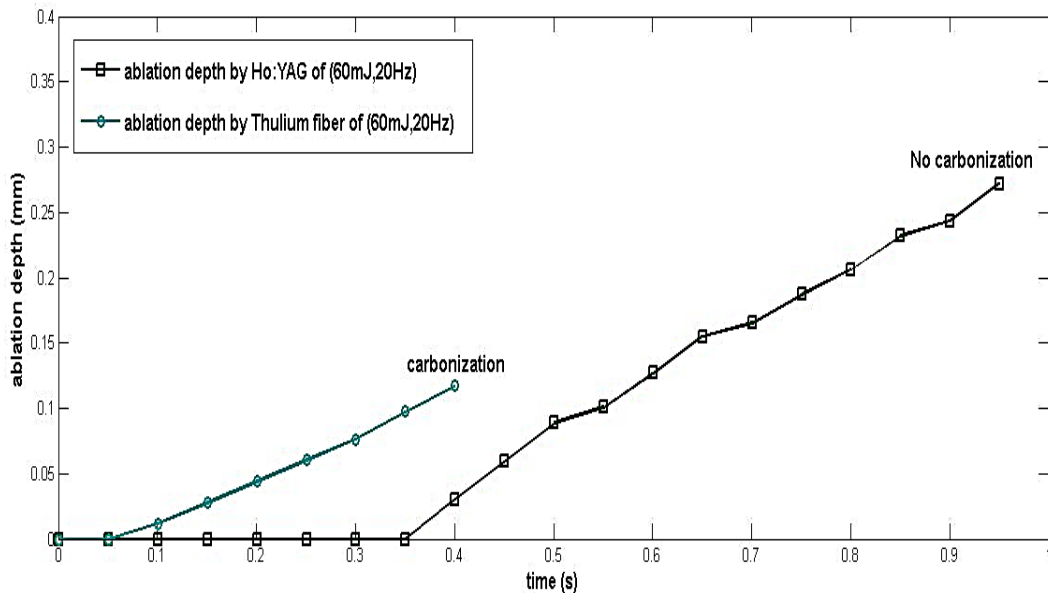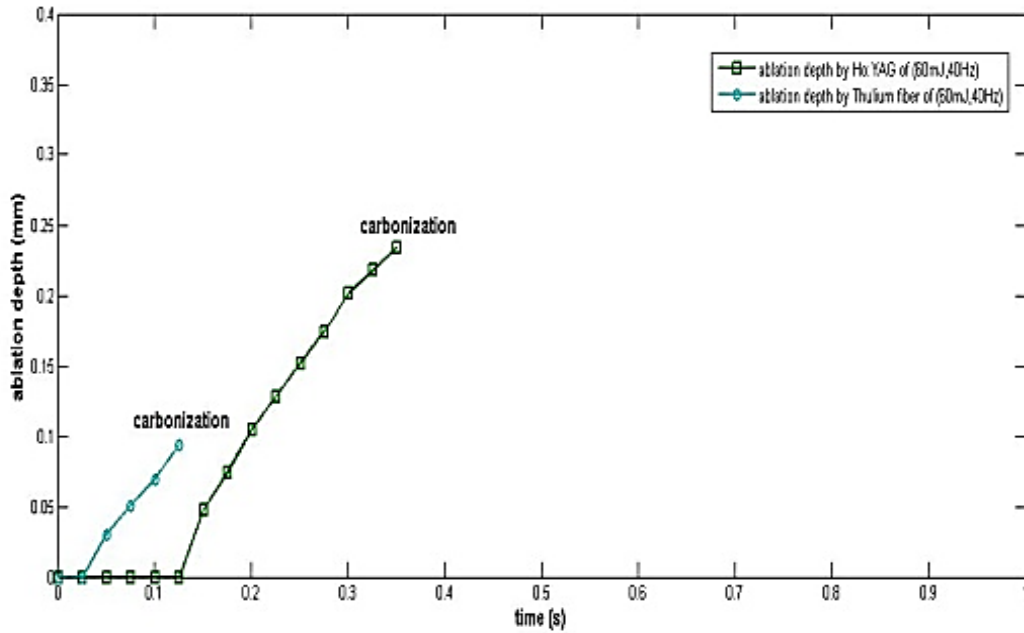**Figure 21:** Ablation depths verses time made by 40 repetition rate and 60 mJ energy for both of pulsed Ho:YAG and Thulium fiber lasers.

.

4. Discussion

The Nd:YAG, Holmium:YAG and the Thulium fiber lasers parameters were used in this mathematical model of simulation, to find out their abilities to ablate the prostate tissue. The ablation required to be clean with minimum carbonization of the surrounding tissue. The prostate absorption coefficients of these lasers energies were the main considered tissue parameter especially for the Ho:YAG and the Thulium fiber lasers. The other effective lasers parameters were their wavelengths; energies and modes of operation (pulsed prf, number of pulses, pulse duration).

The start of ablation considered to start at threshold temperature of 105 C^o. It was found that the required laser energy necessary to rise up the prostate tissue temperature to this threshold value is proportional to the pulse duration of the used lasers as seen in the series of figures (6-9). These figures showed also that the threshold energy for the non carbonization ablation of prostate tissue required for the 1908nm Thulium fiber laser is the lowest compared with the energies required for the 1064 nm Nd:YAG laser or the 2120 nm Ho:YAG laser.

The heat distribution contours within the prostate tissue resulted by the absorption of a single pulse of each of the threshold applied ablation energies, showed that the overheated tissues, which are surrounding the ablated zone is the smallest by using the Thulium fiber laser compared with the single pulse effect of the Nd:YAG or the Ho:YAG lasers, as seen in figures (10, 11 and12).

For the same single pulse durations of these three lasers operating at their threshold energies of ablation, the results showed that the non-carbonization ablation depths of the prostate tissue, which was produced by the Nd:YAG laser is ranged from 0.035 to 0.045mm and the ablation depths produced by the Ho:YAG is ranged from 0.02 to 0.03mm. By using the Thulium fiber the depth is the smallest. It is ranged only from 0.01to 0.020m.The ablation which was produced by the Nd:YAG laser is deeper than the ablation made by the Ho:YAG laser and by the Thulium fiber lasers, but the required energy by the Nd:YAG is the highest as shown by figure (13).

The temperature rise of tissue is not only proportional to the increase of the used energy, but also to the increase of the pulse repetition rate (prf) of a certain laser pulse energy and to its pulse duration. Increasing the prf of the pulsed laser leads to higher rates of temperature rise of the tissue (faster). This means that for higher prf applications the prostate tissue will rapidly reach the carbonization state during the operation process, which is not preferable in surgical operations.

The ablation depth in prostate tissue by using the multi-pulsed Ho:YAG laser is deeper than the ablation depth by the same number of Thulium fiber pulses, before the tissue reaches carbonization, for all of the used energies and repetition rates.

For the same average power delivered to the tissue the Ho:YAG laser showed larger vaporized volume of the prostate tissue at higher rate than the Thulium fiber laser do as shown in figures (16-21). These mathematical simulation results are correspond with the practical surgical results obtained by A.L.Casperson,et.al in 2008 [8].

5. Conclusion

1. The required laser energy to rise up the prostate tissue temperature necessary for ablation is proportional to the laser pulse duration.

2. Thulium fiber laser needs lower energy for ablation than the Holmium and the Nd:YAG lasers for long and short pulses operations. It consequently produce lower side effects like hyperthermia and coagulation in the tissues, which are surrounding the ablated lesion .

3. For a constant used energy the non-carbonized ablation depth is inversely proportional to the pulse duration of the used laser. This depth is the smallest in case of using the Thulium fiber laser.

4. Even though the pulsed Ho:YAG is faster and deeper in ablating the prostate tissue than the Thulium fiber laser do, the Thulium fiber laser is more preferable and safer for surgical applications as it needs lower threshold ablating energy and consequently produce lower side effects like the hyperthermia and coagulation.

References

[1] D.Lo. David, M.A. Mackanos , M.T.Chung, J.S. Hyun, D.T. Montoro, M. Grova, C. Liu, J. Wang, D Palanker, A. J Connolly, M.T. Longaker, C.H. Contag and D.C. Wan, "**Femtosecond plasma mediated laser ablation has advantages over mechanical osteotomy of cranial bone**", Lasers in Surgery and Medicine 44:805–814, 2012.

[2] F. Stelzle, I. Terwey, C. Knipfer, W. Adler, K. T.Gerk, E. Nkenke and M. Schmidt, "**The impact of laser ablation on optical soft tissue differentiation for tissue specific laser surgery-an experimental ex vivo study"** Journal of Translational Medicine, 2012.

[3] D.Albagli,"**Fundamental Mechanisms of Pulsed Laser Ablation of Biological Tissue**", Massachusetts Institute of Technology,1994.

[4] H.J.Foth "**Principles of Lasers**", Willey-VCH Verlag GmbH & Co. KGaA, Weinheim ISBN, 2008.

[5] Adela Ben-Yakar, "**Image-guided ultrafast laser scalpel for precise and minimally invasive surgery",** Conference Paper, CLEO: Science and Innovations,San Jose, California United States,June,Applications of Laser Processing (CM4H), 2013.

[6] J. Jiao, Z. Guo **, " Modeling of ultrashort pulsed laser ablation in water and biological tissues in cylindrical coordinates"**, Applied Physics B: Lasers & Optics, Vol. 103 Issue 1, p195, 2011.

[7] L.C.Wilson and P. J Gilling,"**Lasers for Prostate Surgery – An Update**" ,Business briefing: European Kidney & Urological Aldisease, 2006.

[8] A.L.Casperson, R.A.Barton, N. J. Scott, and N. M. Fried,"**Holmium:YAG (λ = 2120 nm) vs. Thulium Fiber (λ = 1908 nm)Laser for High-Power Vaporization of Canine Prostate Tissue**" ,SPIE Digital Library, 2008.

[9] N.S.Nishioka and Y.Domankevtz, "**Comparison of Tissue Ablation with Pulsed Holmium and Thulium Lasers**", the IEEE Engineering in Medicine and Biology Society,1990.

[10] T.Bilici, Özgür Tabakoğlu, H.Kalaycıoğlu, A.Kurt, A.Sennaroglu, and M.Gülsoy , "**Fluence of Thulium Laser System in Skin Ablation**", IEEE , 2010.

[11] Fluent Inc.(fluent guide), Chapter 13,2006.

[12] M. Esfand Abadi, M. H. Miran Baygi, A. Mahloojifar and S. Moghimi, "**Studying thermal effects of laser on tissue using implicit finite volume method**", Iranian Journal of Electrical & Electronic Engineering, 2005.

[13] M.H.Niemz,"**Laser-Tissue Interaction: Fundamentals and Applications**",Berlin, Heidlberg: Springer–verlag, 2004.

[14] V.V.Barun,A.P.Ivanov,"**Thermal action of a short light pulse on biological tissues**", International Journal of Heat and Mass Transfer, Elsevier Science , 2003.

[15] A.I.Leontiev, N.I.Suslov, E.I.Brekhov and I.u.G.Potapenko,"**Thermophysical regularities of biological effects in tissues**

under the action of concentrated energy fluxes", Doklady AN USSR 310 (in Russian) ,1990.

[16] R.Letfullin, T. F.George, G. C.Duree, and B. M.Bollinger, "Ultrashort Laser Pulse Heating of Nanoparticles: Comparison of Theoretical Approaches", Hindawi Publishing Corporation Advances in Optical Technologies, 2008.

[17] M.A.Mackanos, D.M.Simanovskii, K. E.Schriver, M.S.Hutson, C.H.Contag, J.A.Kozub, and E. D. Jansen, "Pulse Duration Dependent Mid-Infrared Laser Ablation for Biological Applications", IEEE, 2011.

[18] F.F.VÉLEZ and J.L. Arce-Diego,"Light Propagation in Turbid Media: Application to Biological Tissues", IEEE, 2011.

[19] A.Y.Sajjadi a, K.Mitra a, M.Grace , "Ablation of subsurface tumors using an ultra-short pulse laser", Optics and Lasers in Engineering, Science Direct, 2011.

[20] M.M.Jawad, S.T.Abdul Qader, A.A.Zaidan, "An Overview of Laser Principle, Laser-Tissue Interaction Mechanisms and Laser Safety Precautions for Medical Laser Users", International Journal of Pharmacology, 2011.

[21] J. P. Holman, "Heat Transfer", MC Graw Hill, 1981.

[22] M. Cvetkovi´c, D.Poljaky,and A.Perattaz , "Thermal Modelling of the Human Eye Exposed to Laser Radiation",Authorized licensed use limited to: IEEE Xplore, 2012.

[23] .C.Sturesson and S.Anderson-Engels, "A Mathematical Model for Predicting the Temperature Distribution in Laser-Induced Hyperthermia: Exprimental Evaluation and Applications", Phys. Med. Biol. 1995.

دراسة نمذجة استئصال نسيج البروستات بوساطة ليزرات النيوديميوم ـ ياك والهولميوم ياك وليزر ليف الثوليوم النبضية وباقل تاثيرتفحمي

حيدر مناف النعيمي   منقذ سليم داود

وزارة الصحة   قسم الهندسة الطبية

كلية الهندسة، جامعة النهرين

الخلاصة

يعتمد التاثير المتبادل بين الليزر والنسيج الحيوي ومايولده من تاثيرات حرارية على مواصفات كل من النسيج والليزر معا. وفي هذا البحث درست امكانية وكفاءة استئصال نسيج البروستات باستخدام الليزرات النبضية من نوع النيوديميوم ياك والهولميوم ياك وليزر ليف الثوليوم التي تستخدم في العمليات الجراحية. ولهذا الغرض أستخدمت طاقات متعددة من هذه الليزرات في الدراسة وبترددين نبضيين هما 20و40 هرتز لاجل رفع درجة حرارة النسيج الى حد تبخره واستئصاله. لغرض نمذجه هذه العملية استخدم برنامج الكامبت لرسم نموذج هندسي يمثل شكل البروستات ثم أستخدم برنامج الانسس واختيرت معادلات نقل الاشعاع التي تقع ضمن برنامج اخر اسمه الفلونت لحل ونمذجة عملية الاستئصال هذه. وقد اوضحت النتائج التي تم الحصول عليها انه باستخدام الطاقات الواطئة وبترددات تكرار النبضات الواطئة ايضا يزداد الوقت المتاح خلال العملية للحصول على استئصال آمن من دون حدوث تفحم في نسيج البروستات المحيط بمنطقة الاستئصال ووجد ايضا ان ليزر ليف الثوليوم افضل من الليزرين الاخرين في الاستئصال فهو اقل توليدا للتاثيرات الحرارية الجانبية مثل التخثر وفرط الحرارة وتفحم النسيج و ذلك بغض النظر عن كون ليزر الهولميوم ياك اسرع في تبخير النسيج واستئصاله من ليزر ليف الثوليوم.